Structural and physiological neurovascular changes in idiopathic Parkinson's disease and its clinical phenotypes

Sarah Al-Bachari[1,2,3], Rishma Vidyasagar[2,4,5],
Hedley CA Emsley[6,7] and Laura M Parkes[2,8]

Abstract

Neurovascular changes are likely to interact importantly with the neurodegenerative process in idiopathic Parkinson's disease (IPD). Markers of neurovascular status (NVS) include white matter lesion (WML) burden and arterial spin labelling (ASL) measurements of cerebral blood flow (CBF) and arterial arrival time (AAT). We investigated NVS in IPD, including an analysis of IPD clinical phenotypes, by comparison with two control groups, one with a history of clinical cerebrovascular disease (CVD) (control positive, CP) and one without CVD (control negative, CN). Fifty-one patients with IPD (mean age 69.0 ± 7.7 years) (21 tremor dominant (TD), 24 postural instability and gait disorder (PIGD) and six intermediates), 18 CP (mean age 70.1 ± 8.0 years) and 34 CN subjects (mean age 67.4 ± 7.6 years) completed a 3T MRI scan protocol including T_2-weighted fluid-attenuated inversion recovery (FLAIR) and ASL. IPD patients showed diffuse regions of significantly prolonged AAT, small regions of lower CBF and greater WML burden by comparison with CN subjects. TD patients showed lower WML volume by comparison with PIGD patients. These imaging data thus show altered NVS in IPD, with some evidence for IPD phenotype-specific differences.

Introduction

Idiopathic Parkinson's disease (IPD) is the second most common neurodegenerative disorder, for which there are no effective disease modifying or neuroprotective agents. What drives the selective and progressive neuronal dysfunction and loss, the hallmark of neurodegeneration, remains elusive. Neurodegeneration is understood to result from a number of insults or key factors that act and interact over time leading to selective neuronal loss.[1,2] Any of these factors found to be potentially modifiable may point to therapeutic opportunities.

The 'vascular' hypothesis has recently gained much momentum, proposing a key role for neurovascular changes in neuronal dysfunction and loss.[3–7] A number of preclinical studies have identified vascular changes as contributors to the neurodegenerative process, but clinical studies in this area remain equivocal.[8,9] The nature and relevance of vascular changes may also differ between IPD clinical phenotypes perhaps

[1]Department of Neurology, Salford Royal NHS Foundation Trust, Salford, UK
[2]Division of Informatics, Imaging and Data Sciences, School of Health Sciences, Faculty of Biology, Medicine and Health, University of Manchester, Manchester, UK
[3]Faculty of Health and Medicine, Lancaster University, Lancaster, UK
[4]Anatomy and Neuroscience Department, University of Melbourne, Melbourne, Australia
[5]Florey Institute of Neuroscience and Mental Health, Heidelberg, Melbourne, Australia
[6]Department of Neurology, Royal Preston Hospital, Preston, UK
[7]Faculty of Biology, Medicine and Health, University of Manchester, Manchester, UK
[8]Division of Neuroscience and Experimental Psychology, School of Biological Sciences, Faculty of Biology, Medicine and Health, University of Manchester, Manchester, UK

Corresponding author:
Hedley CA Emsley, Department of Neurology, Royal Preston Hospital, Sharoe Green Lane, Fulwood, Preston PR2 9HT, UK.
Email: hedley.emsley@manchester.ac.uk

reflecting pathophysiological differences.[10] Clinical studies often use markers of conventional cerebrovascular disease (CVD), whether clinical (stroke, Transient Ischaemic Attack (TIA)) or imaging (white matter lesion (WML)) which may be insensitive to more subtle neurovascular alterations. Herein we have used the term 'neurovascular status' (NVS) to encompass the various structural and physiological neurovascular markers.

Magnetic resonance imaging (MRI) arterial spin labelling (ASL) is a non-invasive tool which allows quantitative measures of cerebral blood flow (CBF) and arterial arrival time (AAT), the time taken for blood to travel from the labelling slab to the tissue of interest.[11,12] There are numerous studies showing CBF changes in IPD using both ASL[13,14] and other imaging techniques.[15] How and why these occur in the setting of IPD is poorly understood, as is the temporal relationship of CBF changes with neuronal loss. Whether, for instance, atrophic regions merely exhibit secondary hypoperfusion remains debatable.[15] Therefore, measurements of atrophy in addition to CBF are important to determine whether CBF alterations are simply reflective of areas of atrophy or not. AAT is longest in distal branches, especially in border zone (or watershed) areas.[16,17] Alterations in AAT are considered likely to reflect chronic arteriolar vasodilatation, collateral flow and/or increased tortuosity of vessels.[18,19]

Neurovascular alterations have previously been reported in MRI studies of IPD, including our own finding of prolonged AAT.[20] However, little is known about how such changes might vary between clinical IPD phenotypes. In addition, the extent to which such alterations in NVS might either reflect comorbid conventional CVD, or could contribute to, or be a secondary effect of, the neurodegenerative process, is largely unknown.

In this study, we sought to (1) confirm and extend our previous finding of AAT prolongation in IPD, (2) investigate other markers of NVS including WML burden and also measures of brain volume changes (to determine the extent and location of any atrophy) and (3) make comparison between phenotypes and with relevant control groups, including both subjects with and without clinical CVD.

Materials and methods

Approvals, recruitment, eligibility and consent

Relevant approvals were obtained including ethics (North West – Preston Research Ethics Committee), research governance and local university approvals. The study was conducted in accordance with the principles of Good Clinical Practice. Recruitment of IPD patients was from Lancashire Teaching Hospitals (LTH) and Salford Royal Foundation Trust. Eligibility criteria for IPD participants were a clinical diagnosis of IPD fulfilling UK Parkinson's disease society brain bank criteria (http://www.ncbi.nlm.nih.gov/projects) without known clinical CVD (no history of TIA or stroke) or dementia.[21] Participants with CVD were recruited from patients at LTH with a clinical diagnosis of stroke or TIA within the previous two years (at least three months post-onset) supported by relevant brain imaging (control positive, CP). Controls without a history of either IPD or clinical CVD were also recruited (control negative, CN). All groups were matched for age. All participants were required to provide written informed consent and had capacity to do so.

Clinical assessments and phenotyping

IPD phenotype was assessed using the Unified Parkinson's Disease Rating Scale (UPDRS) (http://www.mdvu.org/library/ratingscales/pd/updrs.pdf) during the scan visit. Participants with IPD were classified into three subtypes (tremor dominant (TD), postural instability and gait disorder (PIGD), intermediate) by Jankovic's method.[22] Disease severity was measured using the Hoehn and Yahr rating scale.[23] No alterations were made to the participants' medications for the study protocol. Routine clinical baseline data were also recorded and the levodopa equivalent daily dose (LEDD) calculated.[24] A battery of clinical scales was also administered, including the Montreal Cognitive Assessment (MoCA) (www.MoCAtest.org), details of which are beyond the scope of this paper. Data from participants in an earlier study were included to provide sufficient numbers for phenotypic comparison, comprising 14 patients with IPD and 14 controls scanned on a 3T Philips Achieva MRI system using an eight channel coil at Salford Royal Hospital.[20] Demographics and clinical data were compared between IPD and control participants using unpaired Student's *t*-test with p-value set at < 0.05.

MRI protocol

All participants underwent an approximately 1 h long imaging protocol, on a 3T Philips Achieva MRI system. Twenty-eight participants (14 IPD and 14 CN) were scanned using an eight channel eight head coil at Salford Royal Hospital and the remaining participants using a 32 channel head coil at the Wellcome Trust Clinical Research Facility in Manchester. Involuntary movements in participants were minimised using padding within the head coil. A T_2-weighted

fluid-attenuated inversion recovery image was acquired with the following parameters: TR 11 s, TI 2.8 s, TE 120 ms, in-plane resolution of 0.45 mm, 30 axial slices of 4 mm thickness with 1 mm gap covering the whole brain. A Look-Locker (LL) ASL sequence was used,[25] with STAR labelling[26] and four readout times of 800, 1400, 2000, 2600 ms, TR: 3500 ms; TE 22 ms; flip angle 40°; 3.5 mm × 3.5 mm × 6 mm voxels with 1 mm gap between slices; 15 slices covering the cerebrum but not the cerebellum with bipolar 'vascular crusher' gradients (added to dephase fast flowing spins and so remove large vessel signal). Sixty pairs of label and control images were collected with acquisition time of 7 min. The labelling slab was 15 cm with a 10 mm gap between labelling and imaging regions. To allow quantification of CBF an additional scan was acquired with TR = 10 s and 15 readout times (from 800 to 9200 ms) in order to estimate the equilibrium magnetisation of the brain. A 3D T_1-weighted image with 1 mm isotropic resolution was also collected.

Data analysis

All the data analyses were performed to consider differences between the IPD group as a whole and the CN group (with no history of IPD or clinical CVD), between the IPD group as a whole and the CP group (no history of IPD, but with history of clinical CVD) and between the PIGD and TD groups. These comparisons were selected to establish whether IPD is associated with vascular changes different from those seen in CVD, and whether any such differences vary between clinical IPD phenotypes. In addition, voxel-wise analyses included comparisons between PIGD and CN, and TD and CN, to further investigate regional differences between phenotypes. Voxel-wise analysis of data from the CP group was not considered due to the likely heterogeneous spatial pattern of neurovascular abnormalities.

ASL data were analysed using in-house MATLAB (Mathworks, MA, USA) routines using a single blood compartment model, adapted for LL readout.[20] CBF and AAT maps were calculated and CBF maps were corrected for atrophy using the same method as Johnson et al.,[27] according to the proportion of grey matter (GM) and white matter in each voxel obtained from the segmented T_1-weighted image. Whole brain values for CBF and AAT were calculated using a simple threshold mask based on the ASL control images on an individual basis.

Voxel-wise analysis was also performed using the SPM8 PET toolbox (http://www.fil.ion.ucl.ac.uk/spm/) to determine any regionally specific differences between the groups. The groups were age, but not gender matched, therefore gender was included as a regressor. In addition, all the data were reanalysed using a gender-matched control group. An additional group comparison between the images from the PIGD and TD phenotypes was performed including nuisance covariates of disease severity (UPDRS 111), disease duration and LEDD score to determine the effect of these variables on any phenotypic imaging differences. Image pre-processing in SPM included (1) motion correction, (2) registration and normalisation of the control ASL image to the EPI template within SPM and application of this procedure to the CBF and AAT images and (3) spatial smoothing of the normalised images using an 8 mm full-width-half-maximum kernel. Voxel-wise comparisons of CBF and AAT between the groups were carried out using a two-sample unpaired t-test (unequal variances). Regions were considered significant at a p value < 0.001 uncorrected, with a minimum cluster size of 50 voxels. Further analysis using family-wise error correction for multiple comparisons at the cluster level was performed. The Montreal Neurological Institute (MNI) coordinates were used to locate areas of difference using xjview V 8.14 (http://www.alivelearn.net/xjview8/).

Voxel-based morphometry (VBM) was performed on the T_1-weighted images in SPM8 following standard procedures (http://www.fil.ion.ucl.ac.uk/~john/misc/VBMclass10.pdf), including modulation to allow comparisons of volumes, proportional scaling to individual intracranial volume and smoothing using an 8 mm full width at half maximum (FWHM) kernel.

WML burden was assessed semi-quantitatively using visual rating scales.[28,29] WML volume was also calculated using the lesion segmentation toolbox (LST) in SPM8 with a threshold of 0.3. This threshold was chosen as it gave the most accurate estimates in a sub-study comparing WML volume estimates from LST with those from semi-automated lesion-growing methods on a subset of the data (n = 51, including representation from all groups).[30] Differences between IPD and CN and CP groups for WML burden were measured using the Fazekas periventricular hyperintensity and deep white matter hyperintensity and the Wahlund rating scales. Wahlund and Fazekas scores were stratified into three groups: mild (Wahlund: 0–4; Fazekas: 0–1), moderate (Wahlund: 5–10; Fazekas: 2) and severe (Wahlund: > 10; Fazekas: 3).[31] Fazekas scores were combined into categories (0–1) and 2 where appropriate since the majority of patients scored 1 or 2. The scales were tested using Pearson's Chi squared in SPSS 22, WML volume was compared between the groups using the Mann–Whitney U test in SPSS 22; taking into account the non-parametric nature of the results. Differences were considered significant if p < 0.05.

Finally, the association between imaging findings and MoCA score was assessed by Pearson's correlation.

Results

Participants

Fifty-one IPD patients were recruited (21 TD, 24 PIGD and six intermediates), 18 CP subjects with CVD (14 with ischaemic stroke, four with single or multiple TIAs) (mean time, in years, since diagnosis 1.1 ± 0.7) and 34 CN subjects (Table 1). All groups were matched for age; a difference in gender between the CN group and the other groups was included as a regressor in the ASL analysis. IPD severity and LEDD score varied between the IPD phenotypes, as expected. A greater proportion of PIGD patients were medicated with L-DOPA (92%) compared with TD patients (67%), but DA agonist medication was similar (50% PIGD and 48% TD). MoCA score was significantly lower for the IPD group compared to the CN group ($p < 0.001$) but was similar to the CP group. The PIGD group had significantly lower MoCA score than the TD group ($p < 0.001$).

CBF

Whole brain CBF did not differ significantly between the IPD and CN groups, IPD and CP groups nor between the IPD phenotypes (Figure 1, Table 1).

The voxel-wise analyses did reveal areas of lower CBF in the IPD group by comparison with the CN group, which were predominantly posterior with a few frontal regions (Figure 2, Table 2). There was only one area of higher CBF in the IPD group compared to the CN group, in the right lateral globus pallidus (MNI coordinates [20 −2 4], cluster size 85 voxels, peak t-value 3.7, peak p-value 0.001). The TD and PIGD groups, when compared to the CN group, revealed phenotype-specific patterns of hypoperfusion, with only the PIGD group showing areas of hyperperfusion compared to the CN group (in the right lateral globus pallidus). A direct comparison of the PIGD and TD groups, however, did not reveal any significant difference in CBF, which remained the case when nuisance covariates of disease severity (UPDRS 111), disease duration and LEDD score were included in the analysis. In summary, we found modest reductions in CBF in IPD in comparison to CN, and little difference compared to CP. There were no significant phenotypic differences.

AAT

Whole brain AAT revealed significantly longer AAT in the IPD group as a whole compared to both the CN

Table 1. Demographics, clinical characteristics and whole brain perfusion measures.

	CN (n = 34)	CP (n = 18)	All IPD (n = 51)	P (IPD versus CN)	P (IPD versus CP)	PIGD (n = 24)	TD (n = 21)	P (PIGD versus TD)
Gender (F:M)	18:16	4:14	12:39	n/a	n/a	5:19	7:15	n/a
Age, years (SD); (range)	67.4 (7.6); [52–85]	70.1 (8.0); [53–84]	69.0 (7.7); [52–85]	0.5	0.5	70.0 (7.6); [58–89]	67.9 (7.2); [52–80]	0.3
Cardiovascular risk factors: mean (SD)	1.4 (1.1)	3.1 (1.1)	1.7 (1.5)	0.4	0.0001	1.6 (1.4)	1.8 (1.6)	0.7
Disease duration: mean (SD)	n/a	1.1 (0.7)	7.2 (4.4)	n/a	n/a	9.1 (4.5)	5.1 (3.5)	0.07
Hoehn and Yahr score: mean (SD)	n/a	n/a	2.6 (1.0)	n/a	n/a	3.2 (0.8)	1.8 (0.7)	<0.0001
UPDRS 111 Score: mean (SD)	n/a	n/a	30.2 (11.8)	n/a	n/a	29.9 (21.1)	26.3 (10.8)	0.05
PIGD score: mean (SD)	n/a	n/a	6.8 (4.8)	n/a	n/a	9.2 (4.6)	1.8 (1.5)	n/a
Tremor score: mean (SD)	n/a	n/a	6.2 (5.2)	n/a	n/a	2.8 (3.0)	9.2 (4.6)	n/a
LEDD score (mg): mean (SD)	n/a	n/a	586.4 (336.7)	n/a	n/a	785.9 (310.1)	370.0 (247.8)	<0.0001
MoCA scoremean (SD)	28.0 (2.3)	25.4 (3.3)	25.4 (3.8)	0.0004	1.0	23.8 (3.8)	27.3 (2.7)	0.0008
Whole brain CBF (ml/min/100 ml) $\pm$ SE	46.7 ± 8.8	43.4 ± 7.0	47.5 ± 11.5	1.0	0.06	49.6 ± 13.4	46.7 ± 8.9	0.7
Whole brain AAT (ms) $\pm$ SE	1376 ± 157	1464 ± 134	1525 ± 168	<0.0001	0.04	1507 ± 129	1527 ± 209	0.7

AAT: arterial arrival time; CBF: cerebral blood flow; CN: control negative; CP: control positive; IPD: idiopathic Parkinson's disease; LEDD: levodopa equivalent daily dose; MoCA: Montreal Cognitive Assessment; PIGD: postural instability and gait disorder; TD: tremor dominant; UPDRS 111: unified Parkinson's disease rating scale motor score.
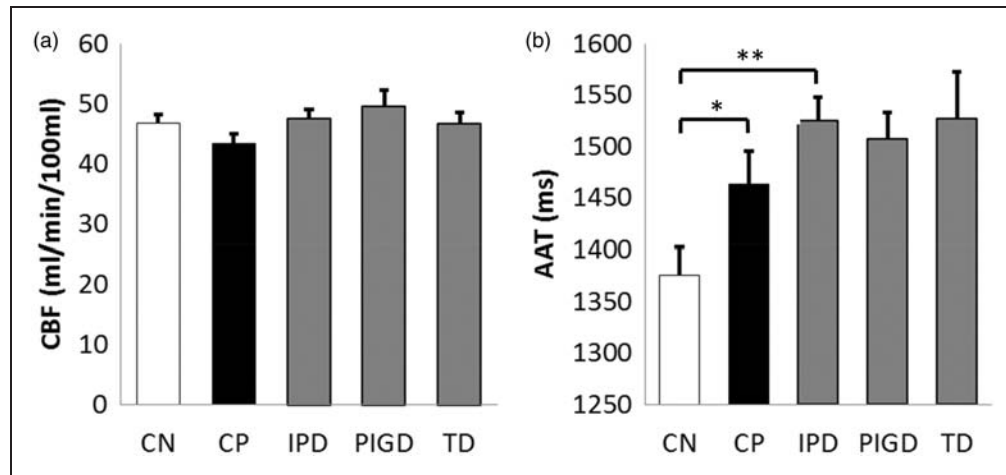
Figure 1. Mean and standard error of whole brain CBF (a) and AAT (b). *p < 0.05, **p < 0.005. AAT: arterial arrival time; CBF: cerebral blood flow.
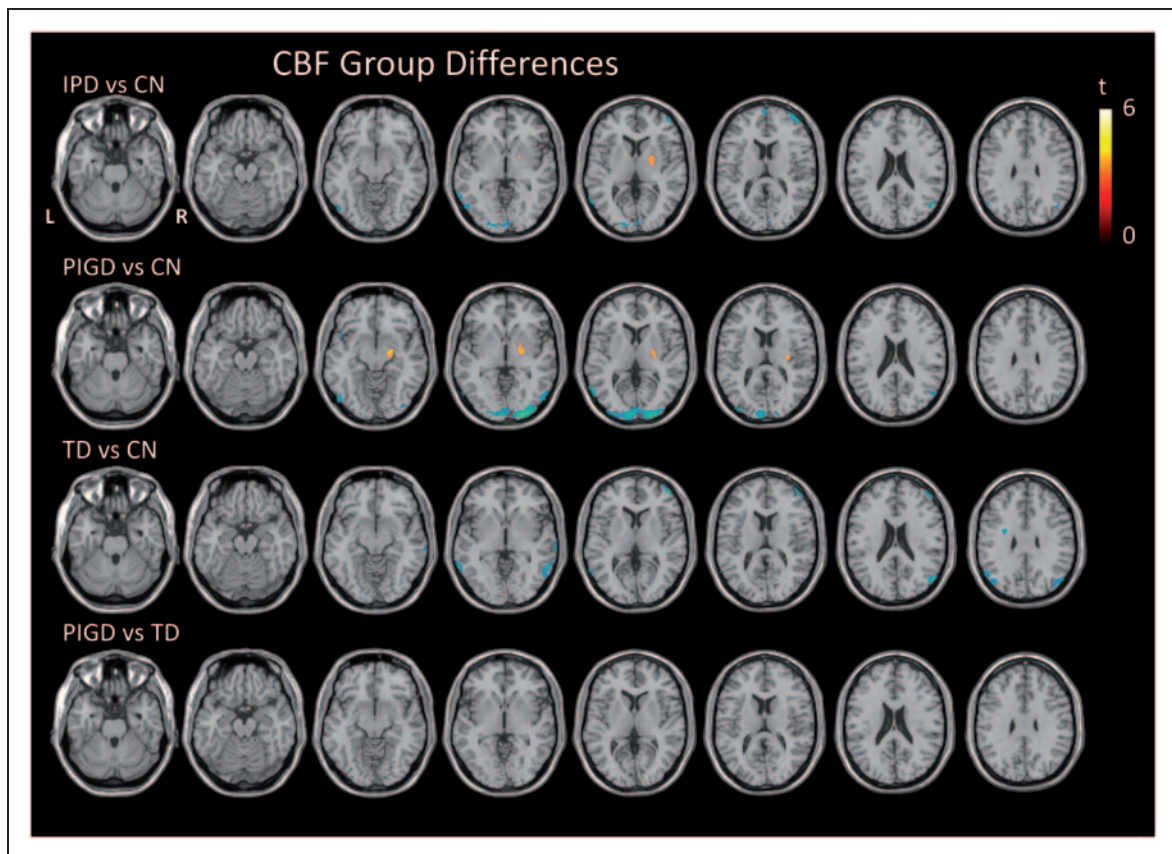

Figure 2. T-statistic maps showing regions of significantly higher (red) and lower (blue) CBF between pairwise group comparisons as indicated, thresholded at p < 0.001 uncorrected, minimum cluster size 50 voxels. CBF: cerebral blood flow.

group (p < 0.005) and the CP group (p < 0.05) (Figure 1, Table 1). No significant differences were observed between IPD phenotypes.

Voxel-wise analyses revealed widespread regions of significantly increased AAT in the IPD group compared to the CN group (Figure 3, Table 3). There were no regions in the brain where AAT was significantly shorter in the IPD group compared to the CN group. The TD group revealed a more diffuse pattern of prolonged AAT than the PIGD group when compared

Table 2. Regions of CBF differences between groups at p < 0.001, cluster size 50 voxels.

Comparison	Region	Cluster Size	Cluster p (FWE corr.)	Peak t value	Peak p (uncorr.)	Peak MNI coordinates
IPD < CN	R middle frontal gyrus	176	0.3	4.6	<0.0001	44 54 12
	L cuneus extending to calcarine region	201	0.2	4.4	<0.0001	−18 −96 2
				3.8	0.0001	2 −94 4
				3.3	0.0008	−8 −98 −4
	L mid temporal gyrus extending to inferior gyrus and occipital region	215	0.2	4.3	<0.0001	−66 −58 4
				3.9	<0.0001	−66 −54 −4
				3.7	0.0002	−60 −66 2
	R mid temporal extending to mid occipital gyrus	96	0.5	4.2	<0.0001	50 −66 24
	R post central gyrus	61	0.6	4.0	<0.0001	32 −36 42
	L precuneus extending to cuneus	358	0.08	4.0	<0.0001	−6 −64 58
				3.9	0.0001	0 −68 48
				3.6	0.0003	−2 −82 40
	L frontal superior medial region	57	0.7	3.9	0.0001	−4 66 12
	L inferior to superior parietal lobule	68	0.6	3.6	0.0003	−30 −72 44
				3.5	0.0004	−54 −66 30
				3.4	0.0005	−46 −64 42
IPD > CN	R lateral globus pallidus	85	0.5	3.9	0.0001	20 −2 4
PIGD < CN	Large region extending most of occipital lobes bilaterally	1540	0.0002	5.9	<0.0001	22 −98 0
				4.6	<0.0001	−8 −100 0
				4.0	<0.0001	−40 −90 18
	L mid temporal to occipital gyrus	102	0.5	4.5	<0.0001	−64 −62 6
	L inferior occipital region	74	0.6	3.9	0.0001	−52 −74 −8
	L superior temporal gyrus	51	0.7	3.7	0.0002	−50 12 −6
				3.6	0.0003	−48 16 −14
	R inferior temporal to inferior occipital region	102	0.5	3.7	0.0002	50 −76 −2
				3.8	0.0002	54 −68 −4
	R mid occipital region	60	0.7	3.7	0.0002	50 −68 26
PIGD > CN	Lentiform nucleus, lateral globus pallidus, putamen and limbic lobe	276	0.1	4.6	<0.0001	20 −12 −12
				4.0	0.0001	20 −6 0
				3.9	0.0001	30 −18 14
TD < CN	R temporal to mid occipital region extending to parietal lobe	276	0.1	4.8	<0.0001	52 −72 24
				3.7	0.0002	40 −78 34
				3.6	0.0003	38 −84 26
	R mid frontal lobe	192	0.3	4.7	<0.0001	46 54 6
				3.8	0.0002	44 52 22
				3.4	0.0002	36 62 14
	Transverse temporal area	76	0.6	4.6	<0.0001	70 −26 −6
	L frontal subgyral region	53	0.7	4.4	<0.0001	−30 −2 32
	L angular region extending to inferior temporal lobule and middle temporal gyrus	364	0.07	4.2	<0.0001	−52 −64 40
				4.0	<0.0001	−46 −72 26
				3.6	0.0003	−42 −78 38
	R middle temporal gyrus	149	0.4	3.6	0.0004	60 −52 0
	L middle temporal gyrus	105	0.5	3.8	0.0002	−64 −60 2
				3.3	0.0008	−66 −52 −2
	L inferior parietal lobule	111	0.5	3.7	0.0001	−58 −38 50
	R subgyral/post central gyrus	75	0.6	3.9	0.0001	26 −42 42

CBF: cerebral blood flow; CN: control negative; FWE: Family-Wise Error; IPD: idiopathic Parkinson's disease; MNI: Montreal Neurological Institute; PIGD: postural instability and gait disorder; TD: tremor dominant.
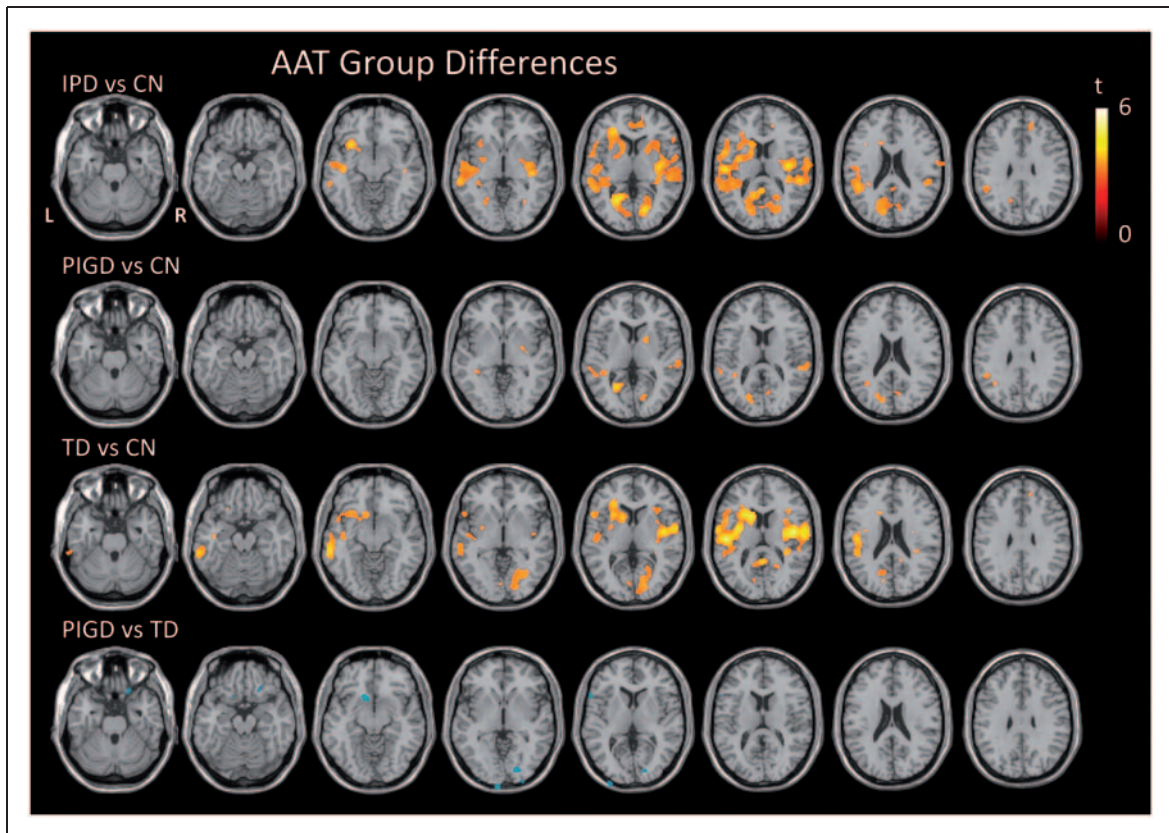
Figure 3. Prolonged AAT in IPD compared to controls. T-statistic maps showing regions of significantly longer (red) and shorter (blue) AAT between pairwise group comparisons as indicated, thresholded at p < 0.001 uncorrected, minimum cluster size 50 voxels. AAT: arterial arrival time; IPD: idiopathic Parkinson's disease.

to the CN group, with a few of these regions reaching significance when directly comparing the TD and PIGD groups. However, no differences between the TD and PIGD groups were observed on direct comparison when nuisance covariates of disease severity (UPDRS 111), disease duration and LEDD score were included in the analysis.

Reanalysis of the data with the gender-matched control group and reanalysis with the removal of the preliminary data (obtained from our earlier study) yielded similar results to those discussed in the above sections.

VBM analysis

The voxel-wise analysis did reveal areas of reduced GM volume in the IPD group as a whole compared to the CN group, predominantly in the temporal lobes (Figure 4). Comparison of TD to PIGD revealed one region of lower GM volume in the TD group in the frontal cortex, but this was no longer significant when nuisance covariates of disease severity (UPDRS 111), disease duration and LEDD score were included in the analysis.

WML burden

All the WML scores were significantly higher in the IPD group as a whole compared to the CN group, with no significant differences between the IPD and CP groups or between the IPD phenotypes.

A trend towards greater WML volume was seen in the IPD group compared to the CN group (p = 0.08). WML volume was significantly higher in the CP group when compared with the IPD group and significantly higher in the PIGD group by comparison with the TD group (Table 4).

Correlations with cognitive impairment

In order to further understand the phenotypic differences in cognitive impairment, we assessed the correlation of individual imaging metrics against MoCA score within the IPD group. We considered WML volume, global AAT and regional CBF values from the regions of hyperperfusion (globus pallidus) and hypoperfusion (predominantly occipital cortex) as identified by the IPD versus CN voxel-wise analysis (Figure 1). Higher WML volume was associated with

Table 3. Regions of AAT differences between groups at p<0.001, cluster size 50 voxels.

Comparison	Region	Cluster size	Cluster p (FWE corr.)	Peak t value	Peak p (uncorr.)	Peak MNI coordinates
IPD > CN	Large region L cerebrum most temporal lobe extending to the insula, parietal and frontal lobes including basal ganglia	7811	<0.0001	5.4 5.2 4.6	<0.0001 <0.0001 <0.0001	16 −74 6 −26 −64 4 −34 18 8
	R cerebrum extending to most temporal lobe, insula, parietal and frontal lobes inc BG	2515	0.0009	4.3 4.1 4.1	<0.0001 <0.0001 <0.0001	36 −12 12 50 −32 12 40 −24 −2
	R cerebrum – limbic and anterior cingulate	410	0.3	4.3 4.1	<0.0001 0.0001	10 44 8 −2 44 6
	R middle and inferior frontal lobe	213	0.6	3.9	<0.0001	10 40 42
	L amygdala	52	0.9	3.7	0.0002	−12 −16 −4
PIGD > CN	L superior to middle temporal gyrus	234	0.5	4.6	<0.0001	−26 −62 2
	L precuneus	190	0.6	4.0	<0.0001	−22 −74 18
	R lentiform nucleus and putamen	110	0.8	4.0 3.7 3.3	0.0001 0.0003 0.0009	18 6 4 26 −6 0 32 −12 −2
	R sup. temporal gyrus	222	0.5	3.9	0.0001	62 −32 12
	L angular gyrus	59	0.9	3.9	0.0002	−38 −56 26
	Sup. and L subgyral temporal lobe	153	0.7	3.8 3.4	0.0002 0.0006	−36 −40 0 −38 −46 16
	L supramarginal	51	0.9	3.7	0.0002	−50 −46 28
	R calcarine	65	0.9	3.7	0.0002	14 −76 6
	L sup temporal gyrus	131	0.8	3.7 3.5	0.0003 0.0004	−62 −34 10 −54 −44 8
	R calcarine	88	0.9	3.7	0.0003	6 −68 18
TD > CN	L post. central gyrus extending to frontal lobe, L insula and superior temporal gyrus, includes L caudate	3386	<0.0001	5.7 5.3 5.0	<0.0001 <0.0001 <0.0001	−52 −18 16 −16 14 12 −34 −4 14
	R insula extends to R precentral gyrus includes R putamen	1709	0.002	5.5 5.0 4.2	<0.0001 <0.0001 <0.0001	42 −8 12 58 −4 10 32 6 10
	R occipital and calcarine extends to R lingual region	976	0.02	4.6 4.1 4.0	<0.0001 <0.0001 <0.0001	0 −50 12 16 −86 2 16 −74 2
	L middle temporal gyrus extending to inferior temporal gyrus	708	0.07	4.5 4.5	<0.0001 <0.0001	−62 −30 −8 −64 −38 −14
	L lingual	67	0.9	3.8	0.0002	−6 −80 2
	L sup. occipital to L cuneus	135	0.7	3.8 3.5	0.0002 0.0004	−18 −64 26 −12 −76 18
	R medial frontal gyrus	74	0.9	3.6 3.6	0.0004 0.0004	12 38 36 10 46 32
TD > PIGD	R calcarine extending to cuneus	91	0.8	4.1	<0.0001	16 −86 2
	L frontal extending to caudate and limbic region	99	0.8	4.1	<0.0001	−14 16 −10
	L inferior frontal gyrus	53	0.9	4.1	<0.0001	−62 18 6
	L mid occipital and calcarine region	68	0.9	4.0	0.0001	−8 −112 −4
	R fronto-superior orbital region extending to R middle frontal gyrus	74	0.9	3.9	0.0002	20 26 −24

Table 3. Continued.

Comparison	Region	Cluster size	Cluster p (FWE corr.)	Peak t value	Peak p (uncorr.)	Peak MNI coordinates
	R middle occipital gyrus extending to calcarine region	52	0.9	3.8	0.0002	26 −102 0
	L mid occipital region	61	0.9	3.7	0.0003	−34 −106 6

AAT: arterial arrival time; CN: control negative; FWE: Family-Wise Error; IPD: idiopathic Parkinson's disease; MNI: Montreal Neurological Institute; PIGD: postural instability and gait disorder; TD: tremor dominant.
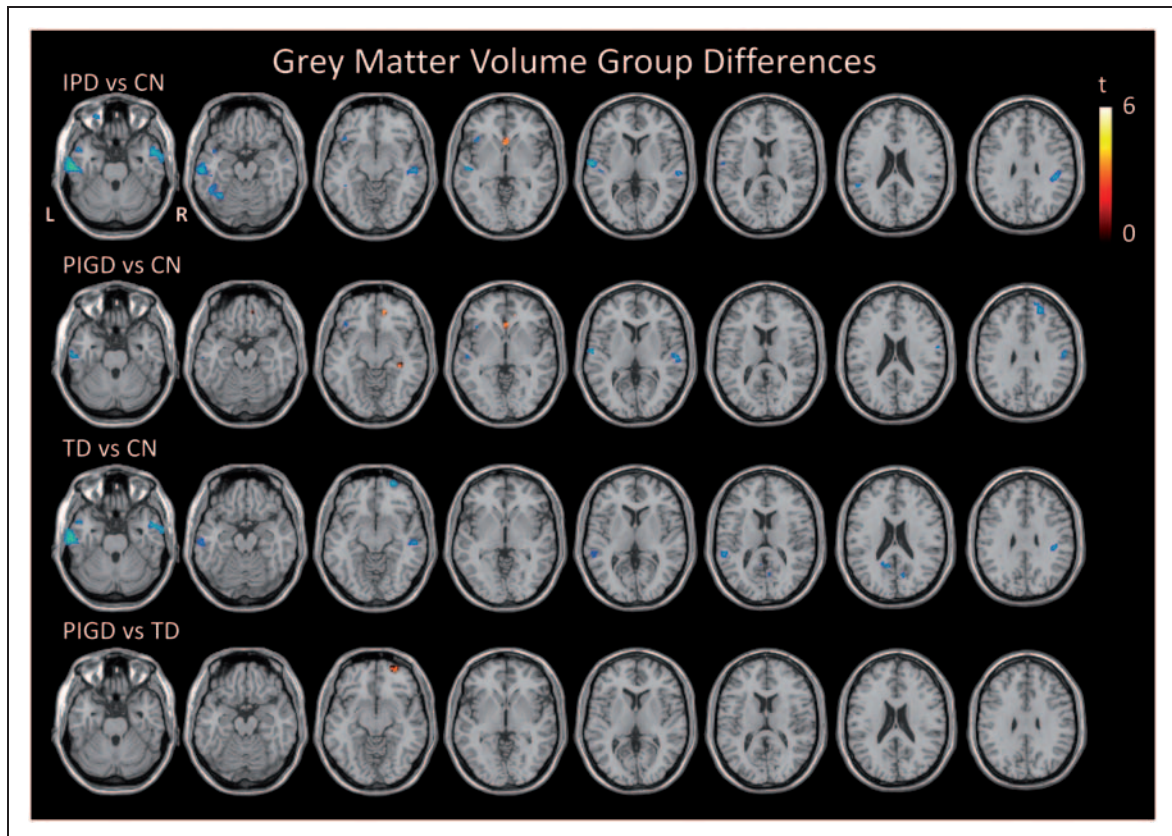

Figure 4. T-statistic maps showing regions of significantly greater (red) and less (blue) grey matter volume between pairwise group comparisons as indicated, thresholded at p < 0.001 uncorrected, minimum cluster size 50 voxels.

lower MoCA score (r=−0.39, p = 0.005) across the IPD group and this association remained significant within the TD group (TD r = −0.45, p = 0.03, PIGD r = −0.29, p = 0.2). However, there was no association between AAT and MoCA score (r = −0.16, p = 0.3) or CBF and MoCA score (hyperperfused region r = −0.2, p = 0.20, hypoperfused region r = 0.005, p = 1.0).

Discussion

This study used a multimodal MRI approach in a clinical study to better understand NVS in IPD and revealed key differences in NVS, namely AAT prolongation, reduced CBF and differences in WML burden in IPD patients by comparison with age-matched controls with and without CVD. Within the IPD group phenotype-specific differences were also revealed.

This study confirmed our previous findings of diffuse prolonged AAT in IPD patients compared to controls; whole brain analysis revealed this prolongation to be greater in IPD patients than in controls both with and without CVD. As the IPD group had significantly fewer vascular risk factors than the CP group, this raises the interesting possibility that mechanisms of AAT prolongation might be independent of, or at the least

Table 4. WML rating scales and volumes (p value Pearson's Chi squared for rating scales and Mann–Whitney for WML volume).

	CN (n = 34)	CP (n = 18)	All IPD (n = 51)	p value (IPD versus CN)	p value (IPD versus CP)	PIGD (n = 24)	TD (n = 21)	p value (PIGD versus TD)
Wahlund Score: N(%)								
Mild	23 (67.6)	3 (16.7%)	17 (33.3)	0.005	0.3	6 (25.0%)	8 (38.1%)	0.6
Moderate	9 (26.5)	12 (66.7%)	23 (45.1)			13 (54.2%)	8 (38.1%)	
Severe	2 (5.9)	3 (16.7%)	11 (21.6)			5 (20.8%)	5 (23.8%)	
Fazekas PVH: N(%)								
(0–1) Mild	25 (73.5)	5 (27.8%)	22 (43.1)	0.02	0.4	8 (33.3%)	11 (52.4%)	0.5
(2) Moderate	6 (17.6%)	10 (55.6%)	20 (39.2)			12 (50%)	7 (33.3%)	
(3) Severe	3 (8.8%)	3 (16.7%)	9 (17.6)			4 (16.7%)	3 (14.3%)	
Fazekas DWMH: N(%)								
(0–1) Mild	28 (82.4%)	11 (61.1%)	27 (52.9)	0.02	0.9	10 (41.7%)	14 (66.7%)	0.2
(2) Moderate	4 (11.8%)	5 (27.8%)	18 (35.3)			11 (45.8%)	5 (23.8%)	
(3) Severe	2 (5.9%)	2 (11.1%)	6 (11.8)			3 (12.5%)	2 (9.5%)	
WML Volume: (ml)								
Median (IR)	1.41 (3)	10.44 (15)	4 (9)	0.08	<0.001	8.03 (15)	1 (4)	<0.001

CN: control negative; CP: control positive; DWMH, deep white matter hyperintensity; IPD: idiopathic Parkinson's disease; PIGD: postural instability and gait disorder; PVH, periventricular hyperintensity; TD: tremor dominant; WML: white matter lesion.

driven by other factors than, conventional CVD. The prolonged AAT appeared more diffuse in the TD compared to PIGD group (Figure 3), and this may be related to the shorter disease duration and lower disease severity in TD compared to PIGD as voxel-wise differences were no longer seen on direct comparison when these factors were taken into account. Given that the TD phenotype is generally considered to have a more benign clinical course, it might be inferred that prolongation of AAT appears somewhat 'protective'.

Indeed AAT has been measured in acute stroke studies revealing areas of prolonged AAT generally reflecting preserved perfusion, lack of progression to infarct and more minor symptoms.[32–34] Prolonged AAT has been postulated to be reflective of recruitment of collaterals[33,35] or secondary to altered vasculature causing a decrease in the flow velocity, for example, increased tortuosity, altered vascular wall diameter/compliance and chronic vasodilation.[36–39]

WML burden, as measured by visual rating scales, was higher in the IPD patients than in the CN subjects – in keeping with our earlier work.[9] WML rating scales also revealed a greater burden in CP than IPD which is to be expected yet also suggests conventional CVD may not be driving AAT prolongation. Of note WML volume (arguably a more accurate measure of WML burden as rating scales do not take into account the size/volume of the lesions) was significantly higher in the PIGD than in the TD group, indeed PIGD WML volumes were comparable control subjects with CVD. This strengthens the case for a differential pattern of changes in NVS between IPD phenotypes. WML volume showed a significant association with MoCA score showing the influence of WML volume on cognitive impairment, unlike the other imaging metrics which were not associated with cognitive impairment. One possible interpretation might be that WMLs reflect established structural tissue damage, whereas alterations in AAT and CBF reflect functional vascular changes.

CBF differences between the IPD group and CN are in keeping with other imaging studies.[13,14,40,41] For example, quantitative studies using PET have previously shown PD to be characterised by both hypoperfusion and hypometabolism in widespread cortical regions, particularly in frontal and parietal cortical regions, with occipital cortices probably more affected than the temporal cortex, and possibly also in some subcortical structures.[15] The PIGD group had a more predominantly posterior pattern of hypoperfusion and indeed basal ganglia hyperperfusion than the more temporo-parieto-frontal hypoperfusion of the TD group (which did not show areas of hyperperfusion). To the authors' knowledge the IPD phenotype differences revealed in this study have not been previously investigated. The noticeable pattern of hypoperfusion of the PIGD group, in the occipital cortex, encompassing the primary visual cortex, believed to be involved in gait and the more frontal TD regions felt to be involved in tremor[42] may reflect differences in pathophysiology between IPD phenotypes and warrants further investigation. The region of hyperperfusion in the globus pallidus in patients is in keeping with previous findings of elevated glucose metabolism in this region.[43] However, it may also be related to L-DOPA medication which has been shown to increase CBF in this region,[44,45] particularly as the hyperperfusion is greatest in the PIGD group of whom a greater proportion were on L-DOPA medication (Table 1).

Some would argue that perfusion changes are simply secondary to neuronal loss, if that were the case then one would expect a similar anatomical distribution of GM loss demonstrated by VBM to that of the reduction in perfusion, yet they are clearly distinct, with GM loss restricted to the temporal lobes. Interestingly, studies in AD at the preclinical stages and even in relatives of those with AD have revealed early perfusion changes:[46,47] this may suggest that some changes in perfusion in neurodegenerative states occur before neuronal loss. This raises an interesting hypothesis to be tested in IPD – that perfusion changes are a forerunner to, rather than a sequel of, neuronal loss. One possible mechanism is the impact of perfusion alterations on the regulation of brain metabolism, as there is a close relationship between neurovascular and metabolic changes. For example, decreased mitochondrial electron transport chain activity has been implicated in PD pathogenesis, and there is some evidence to support the occurrence of parallel declines in the rate of cerebral oxygen consumption ($CMRO_2$), glucose utilisation (CMRglc) and CBF in spatially contiguous cortical regions in early PD.[48] There is a need for prodromal studies (e.g. in specific individuals with genetic predisposition) and longitudinal studies temporally mapping vascular and neuronal changes.

Although we have investigated potential differences between PIGD and TD, in the present study PIGD patients had greater disease severity and higher LEDD score. When account was taken of this in the analysis, voxel-wise phenotypic differences in AAT did not persist. This may be in keeping with other recent observations using ASL MRI in patients with PD and PD dementia (PDD), which found widespread cortical hypoperfusion and further reductions in frontal lobe and cerebellum perfusion in PD and PDD, respectively, with dopaminergic medication.[49] The observed patterns of hypoperfusion in this study were thought to potentially relate to cognitive dysfunction and disease severity.

Aside from imaging, other studies reveal evidence of neurovascular changes in PD, supporting our findings. For example, CSF biomarkers of angiogenesis have been found to be increased in PD, and to be associated with gait difficulties, increased BBB permeability, WMLs and cerebral microbleeds, indicating that abnormal angiogenesis may be relevant to PD pathogenesis and contribute to dopa-resistant symptoms.[50] Other lines of evidence include pathological study of human PD cases showing endothelial degeneration and preservation of basement membrane leading to an increase of string vessel formation in PD. String vessels have no function in circulation, and this suggests a possible role for cerebral hypoperfusion in the neuronal degeneration characteristic of PD.[51]

The main limitations to this study are that certain variables could not be controlled for including LEDD, disease duration and disease severity and these were found to differ between the disease phenotypes. To evaluate their potential impact they were included as nuisance covariates in the voxel-wise AAT and CBF comparisons. This resulted in removal of phenotypic imaging differences, suggesting that these imaging differences are driven in part by these factors.

Conclusion

This study has confirmed and added to our previous findings; namely, there is diffuse prolongation of AAT and reduced CBF in IPD patients by comparison with normal control subjects, and prolonged global AAT in IPD patients by comparison with controls subjects with CVD, despite significantly fewer vascular risk factors. TD patients showed lower WML volume by comparison with PIGD patients. These imaging data thus show altered NVS in IPD, with some evidence for IPD phenotype-specific differences. Further studies are needed, likely longitudinal, to further investigate possible differences in the neurovascular contribution to the pathophysiology of particular IPD phenotypes, and to establish whether neurovascular changes partly drive, or are secondary to, the neurodegenerative process.

Declaration of conflicting interests

The author(s) declared no potential conflicts of interest with respect to the research, authorship, and/or publication of this article.

Authors' contributions

References

1. Bourdenx M, Dovero S, Engeln M, et al. Lack of additive role of ageing in nigrostriatal neurodegeneration triggered by alpha-synuclein overexpression. *Acta Neuropathol Commun* 2015; 3: 46.
2. Collins LM, Toulouse A, Connor TJ, et al. Contributions of central and systemic inflammation to the pathophysiology of Parkinson's disease. *Neuropharmacology* 2012; 62: 2154–2168.
3. Grammas P, Martinez J and Miller B. Cerebral microvascular endothelium and the pathogenesis of neurodegenerative diseases. *Expert Rev Mol Med* 2011; 13: e19.
4. Nelson AR, Sweeney MD, Sagare AP, et al. Neurovascular dysfunction and neurodegeneration in dementia and Alzheimer's disease. *Biochim Biophys Acta* 2016; 1862: 887–900.
5. Sagare AP, Bell RD and Zlokovic BV. Neurovascular dysfunction and faulty amyloid beta-peptide clearance in Alzheimer disease. *Cold Spring Harb Perspect Med* 2012; 2: a011452.
6. Zhao Z, Nelson AR, Betsholtz C, et al. Establishment and dysfunction of the blood-brain barrier. *Cell* 2015; 163: 1064–1078.
7. Zlokovic BV. The blood-brain barrier in health and chronic neurodegenerative disorders. *Neuron* 2008; 57: 178–201.
8. Nanhoe-Mahabier W, de Laat KF, Visser JE, et al. Parkinson disease and comorbid cerebrovascular disease. *Nat Rev Neurol* 2009; 5: 533–541.
9. Patel M, Coutinho C and Emsley HC. Prevalence of radiological and clinical cerebrovascular disease in idiopathic Parkinson's disease. *Clin Neurol Neurosurg* 2011; 113: 830–834.
10. Thenganatt MA and Jankovic J. Parkinson disease subtypes. *JAMA Neurol* 2014; 71: 499–504.
11. Wang J, Alsop DC, Song HK, et al. Arterial transit time imaging with flow encoding arterial spin tagging (FEAST). *Magn Reson Med* 2003; 50: 599–607.
12. Zappe AC, Reichold J, Burger C, et al. Quantification of cerebral blood flow in nonhuman primates using arterial spin labeling and a two-compartment model. *Magn Reson Imaging* 2007; 25: 775–783.
13. Fernandez-Seara MA, Mengual E, Vidorreta M, et al. Cortical hypoperfusion in Parkinson's disease assessed using arterial spin labeled perfusion MRI. *NeuroImage* 2012; 59: 2743–2750.
14. Melzer TR, Watts R, MacAskill MR, et al. Arterial spin labelling reveals an abnormal cerebral perfusion pattern in Parkinson's disease. *Brain* 2011; 134: 845–855.
15. Borghammer P. Perfusion and metabolism imaging studies in Parkinson's disease. *Dan Med J* 2012; 59: B4466.

16. Hendrikse J, Petersen ET, van Laar PJ, et al. Cerebral border zones between distal end branches of intracranial arteries: MR imaging. *Radiology* 2008; 246: 572–580.
17. Petersen ET, Zimine I, Ho YC, et al. Non-invasive measurement of perfusion: a critical review of arterial spin labelling techniques. *Br J Radiol* 2006; 79: 688–701.
18. Derdeyn CP, Videen TO, Yundt KD, et al. Variability of cerebral blood volume and oxygen extraction: stages of cerebral haemodynamic impairment revisited. *Brain* 2002; 125: 595–607.
19. Farkas E and Luiten PG. Cerebral microvascular pathology in aging and Alzheimer's disease. *Prog Neurobiol* 2001; 64: 575–611.
20. Al-Bachari S, Parkes LM, Vidyasagar R, et al. Arterial spin labelling reveals prolonged arterial arrival time in idiopathic Parkinson's disease. *Neuroimage Clin* 2014; 6: 1–8.
21. Emre M, Aarsland D, Brown R, et al. Clinical diagnostic criteria for dementia associated with Parkinson's disease. *Mov Disord* 2007; 22: 1689–1707.
22. Jankovic J, McDermott M, Carter J, et al. Variable expression of Parkinson's disease: a base-line analysis of the DATATOP cohort. The Parkinson Study Group. *Neurology* 1990; 40: 1529–1534.
23. Hoehn MM and Yahr MD. Parkinsonism: onset, progression and mortality. *Neurology* 1967; 17: 427–442.
24. Tomlinson CL, Stowe R, Patel S, et al. Systematic review of levodopa dose equivalency reporting in Parkinson's disease. *Mov Disord* 2010; 25: 2649–2653.
25. Gunther M, Bock M and Schad LR. Arterial spin labeling in combination with a look-locker sampling strategy: inflow turbo-sampling EPI-FAIR (ITS-FAIR). *Magn Reson Med* 2001; 46: 974–984.
26. Edelman RR, Siewert B, Darby DG, et al. Qualitative mapping of cerebral blood flow and functional localization with echo-planar MR imaging and signal targeting with alternating radio frequency. *Radiology* 1994; 192: 513–520.
27. Johnson NA, Jahng GH, Weiner MW, et al. Pattern of cerebral hypoperfusion in Alzheimer disease and mild cognitive impairment measured with arterial spin-labeling MR imaging: initial experience. *Radiology* 2005; 234: 851–859.
28. Fazekas F, Kleinert R, Offenbacher H, et al. Pathologic correlates of incidental MRI white matter signal hyperintensities. *Neurology* 1993; 43: 1683–1689.
29. Wahlund LO, Barkhof F, Fazekas F, et al. A new rating scale for age-related white matter changes applicable to MRI and CT. *Stroke* 2001; 32: 1318–1322.
30. Schmidt P, Gaser C, Arsic M, et al. An automated tool for detection of FLAIR-hyperintense white-matter lesions in multiple sclerosis. *NeuroImage* 2012; 59: 3774–3783.
31. Leonards CO, Ipsen N, Malzahn U, et al. White matter lesion severity in mild acute ischemic stroke patients and functional outcome after 1 year. *Stroke* 2012; 43: 3046–3051.
32. Chalela JA, Alsop DC, Gonzalez-Atavales JB, et al. Magnetic resonance perfusion imaging in acute ischemic

stroke using continuous arterial spin labeling. *Stroke* 2000; 31: 680–687.

33. MacIntosh BJ, Lindsay AC, Kylintireas I, et al. Multiple inflow pulsed arterial spin-labeling reveals delays in the arterial arrival time in minor stroke and transient ischemic attack. *Am J Neuroradiol* 2010; 31: 1892–1894.

34. Wolf ME, Layer V, Gregori J, et al. Assessment of perfusion deficits in ischemic stroke using 3D-GRASE arterial spin labeling magnetic resonance imaging with multiple inflow times. *J Neuroimaging* 2014; 24: 453–459.

35. Zaharchuk G. Arterial spin label imaging of acute ischemic stroke and transient ischemic attack. *Neuroimaging Clin N Am* 2011; 21: 285–301.

36. Liu Y, Zhu X, Feinberg D, et al. Arterial spin labeling MRI study of age and gender effects on brain perfusion hemodynamics. *Magn Reson Med* 2012; 68: 912–922.

37. MacIntosh BJ, Swardfager W, Robertson AD, et al. Regional cerebral arterial transit time hemodynamics correlate with vascular risk factors and cognitive function in men with coronary artery disease. *AJNR Am J Neuroradiol* 2015; 36: 295–301.

38. Paling D, Thade Petersen E, Tozer DJ, et al. Cerebral arterial bolus arrival time is prolonged in multiple sclerosis and associated with disability. *J Cereb Blood Flow Metab* 2014; 34: 34–42.

39. Detre JA and Alsop DC. Perfusion magnetic resonance imaging with continuous arterial spin labeling: methods and clinical applications in the central nervous system. *Eur J Radiol* 1999; 30: 115–124.

40. Kamagata K, Motoi Y, Hori M, et al. Posterior hypoperfusion in Parkinson's disease with and without dementia measured with arterial spin labeling MRI. *J Magn Reson Imaging* 2011; 33: 803–807.

41. Nobili F, Arnaldi D, Campus C, et al. Brain perfusion correlates of cognitive and nigrostriatal functions in de novo Parkinson's disease. *Eur J Nucl Med Mol Imaging* 2011; 38: 2209–2218.

42. Mure H, Hirano S, Tang CC, et al. Parkinson's disease tremor-related metabolic network: characterization, progression, and treatment effects. *NeuroImage* 2011; 54: 1244–1253.

43. Huang C, Tang C, Feigin A, et al. Changes in network activity with the progression of Parkinson's disease. *Brain* 2007; 130: 1834–46.

44. Hirano S, Asanuma K, Ma Y, et al. Dissociation of metabolic and neurovascular responses to levodopa in the treatment of Parkinson's disease. *J Neurosci* 2008; 28: 4201–4209.

45. Leenders KL, Wolfson L, Gibbs JM, et al. The effects of L-DOPA on regional cerebral blood flow and oxygen metabolism in patients with Parkinson's disease. *Brain* 1985; 108: 171–191.

46. Okonkwo OC, Xu G, Oh JM, et al. Cerebral blood flow is diminished in asymptomatic middle-aged adults with maternal history of Alzheimer's disease. *Cereb Cortex* 2014; 24: 978–988.

47. Wierenga CE, Hays CC and Zlatar ZZ. Cerebral blood flow measured by arterial spin labeling MRI as a preclinical marker of Alzheimer's disease. *J Alzheimers Dis* 2014; 42: S411–419.

48. Borghammer P, Cumming P, Østergaard K, et al. Cerebral oxygen metabolism in patients with early Parkinson's disease. *J Neurol Sci* 2012; 313: 123–128.

49. Lin WC, Chen PC, Huang YC, et al. Dopaminergic therapy modulates cortical perfusion in Parkinson Disease with and without dementia according to arterial spin labeled perfusion magnetic resonance imaging. *Medicine (Baltimore)* 2016; 95: e2206.

50. Janelidze S, Lindqvist D, Francardo V, et al. Increased CSF biomarkers of angiogenesis in Parkinson disease. *Neurology* 2015; 85: 1834–1842.

51. Yang P, Pavlovic D, Waldvogel H, et al. String vessel formation is increased in the brain of Parkinson Disease. *J Parkinsons Dis* 2015; 5: 821–836.